Studied Sections

We investigated the Upper Barremian-Lower Aptian interval recovered at two drill sites: the Cismon core and DSDP Site 463 in the Mid-Pacific Mountains.

The Cismon drill site is located in the Southern Alps (north-eastern Italy) (46°02´N; 11°45´E; 398 m altitude). The site was located on the continental margin of the Mesozoic Tethys, on the eastward deepening slope between the Trento Plateau and the Belluno Basin (Fig. DR1). The Cismon sequence was deposited at an estimated paleo-depth of 1000-1500 m during the Early Cretaceous (Weissert and Lini, 1991; Erba and Larson 1998; Bernoulli and Jenkyns, 2009). The Selli level is represented by a ~5m-thick layer of hemipelagic sediments, between 23.67 and 18.64 stratigraphic meter depths (Erba and Larson, 1998; Erba et al., 1999). Lithologically the Selli level is characterized by marlstone alternating with black shales and discrete radiolarian beds (Erba et al., 1999).

DSDP Site 463 was drilled at a water depth of 2525 m in the ancient structural high of the western Mid-Pacific Mountains (21°21.01′N, 174°40.07′E). During the Early Cretaceous, Site 463 was located at a paleo-latitude of ~20ºS (Fig. DR1), with a paleo-depth between a few hundred meters (Mélières et al., 1978) and ~1 km (Roth, 1981). The Selli level at DSDP Site 463 is located between ~626-615 mbsf, corresponding to ~12 m of tuffaceous limestone containing a number of discrete organic-rich horizons with TOC up to 7 (wt%) (Thiede et al., 1981; Erba, 1994).

Methods

We selected for analysis 27 samples from the Cismon core and 32 samples from DSDP Site 463 from an interval covering the Upper Barremian-Lower Aptian. We chose, where possible, black shale layers or organic rich samples (on the basis of their TOC content).

1. <u>Re–Os isotope analyses</u>

Rhenium and osmium abundance data and Os-isotope compositions were determined on ~0.5 g aliquots of powdered rock; analyses were performed at The Open University. Initial digestion took place using 12 ml of inverse aqua regia (3:1 mixture of conc. HNO_3 and conc. HCl) in sealed Carius tubes at 180°C for 5 days, broadly following the methods of Cohen and Waters (1996).

Os was extracted into CCl_4 (Cohen and Waters, 1996), and Re (in inverse aqua regia) was extracted into isoamylol. From the CCl_4, Os was back extracted into HBr and purified by micro-distillation (following Roy-Barman and Allegre, 1995) using CrO_3 in H_2SO_4 as oxidizing agent. Re and Os isotope ratio and abundance determinations were performed on a Thermo-Finnigan Triton high resolution multicollector mass spectrometer operated in N-TIMS mode (Cohen and Waters, 1996).

Each batch of samples was analysed along with aliquots of an in-house mudrock standard and with appropriate Re and Os solution standards. Repeat measurements of a DTM Os solution standard yielded long-term $^{187}Os/^{188}Os$ reproducibility < 0.2% (2 s.d.), with a mean $^{187}Os/^{188}Os = 0.17390 \pm 0.00014$ (n = 32) over the period when the sample measurements were made.

All data were corrected for procedural blanks, amounting to 0.3-0.68 ppt for Os and 3.8 ppt for Re. The Os-isotope composition of seawater ($^{187}Os/^{188}Os$) was calculated from the analyses of individual samples assuming the Re–Os system became closed soon after sediment deposition (Tables DR1, DR2, DR3). Re–Os isotope regressions were calculated using *Isoplot3.0* (Ludwig, 1998).

The initial Os-isotope ratios ($^{187}Os/^{188}Os_{(i)}$) were calculated assuming an age of 120 Ma for the Selli interval, based on cyclochronology for the Cismon core (Malinverno et al., 2010). We note that an age of 125 Ma was used by Tejada et al. (2009) for the samples that they analysed from Gorgo a Cerbara. The discrepancy in $^{187}Os/^{188}Os_{(i)}$ is, however, negligible (as indicated in Table DR5) when comparing the calculated values.

The exceptionally unradiogenic Os isotope compositions that characterise segment D (Fig. 1) are fully consistent with a large additional flux of unradiogenic Os from the hydrothermal alteration of OJP basalts. We assume a total volume for the OJP of $2x10^7$ km^3, with an Os concentration of 50 ppt and a rock density of 3 g/cm^3 (note that the Os abundance in pristine OJP lavas is relatively high, with measured values between 20 and 160 ppt – I. J. Parkinson, pers. comm.). The total mass of basalt emplaced was $6x10^{19}$ kg and the total Os inventory in this basalt would have been $3x10^9$ kg, which is well over 2 orders of magnitude greater than the estimated present-day seawater Os budget of $1.4x10^7$ kg.

2. <u>Elemental analyses</u>

The concentrations of total organic carbon (TOC) wt%, calcium carbonate ($CaCO_3$) wt%, total nitrogen (N) and total sulphur (S) were determined on aliquots of the Cismon samples (Table DR2) using a LECO Instruments CNS-2000 elemental analyser at The Open University.

3. <u>Carbon stable-isotope analyses</u>

Carbon stable-isotope analyses were performed at Oxford University on bulk carbonate and organic-carbon fraction of 57 samples from DSDP Site 463. Long-term reproducibility, as determined from repeat measurements of our working standard, resulted in analytical uncertainties of $\delta^{13} C_{carb}= 2.09 \pm 0.07$, $\delta^{13} C_{org}= -26.91 \pm 0.11$(n=16); see Table DR4.

The values are reported in the conventional delta notation with respect to the Vienna Pee Dee Belemnite (V-PDB) standard (1):

$$\delta^{13}C_{sample}=\{[(^{13}C/^{12}C)_{sample}/(^{13}C/^{12}C)_{reference}]-1\}*1000 \qquad (1)$$

Analyses on the organic carbon fraction were performed on 2 g of powdered sample after sample decarbonation in 3M HCl.

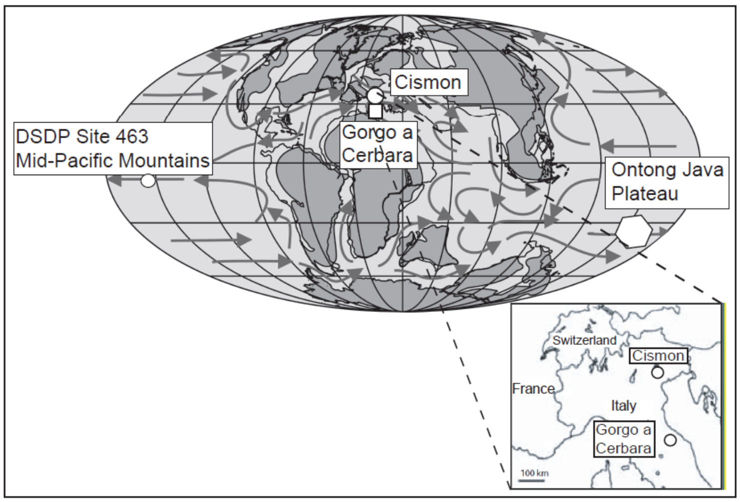

Figure DR1. Palaeogeographic reconstruction and proposed oceanic circulation at 100 Ma (Hay, 2009). Location of DSDP Site 463 (Mid-Pacific Mountains), the Cismon drill site, and the Gorgo a Cerbara section are shown in relation to the Ontong Java Plateau.

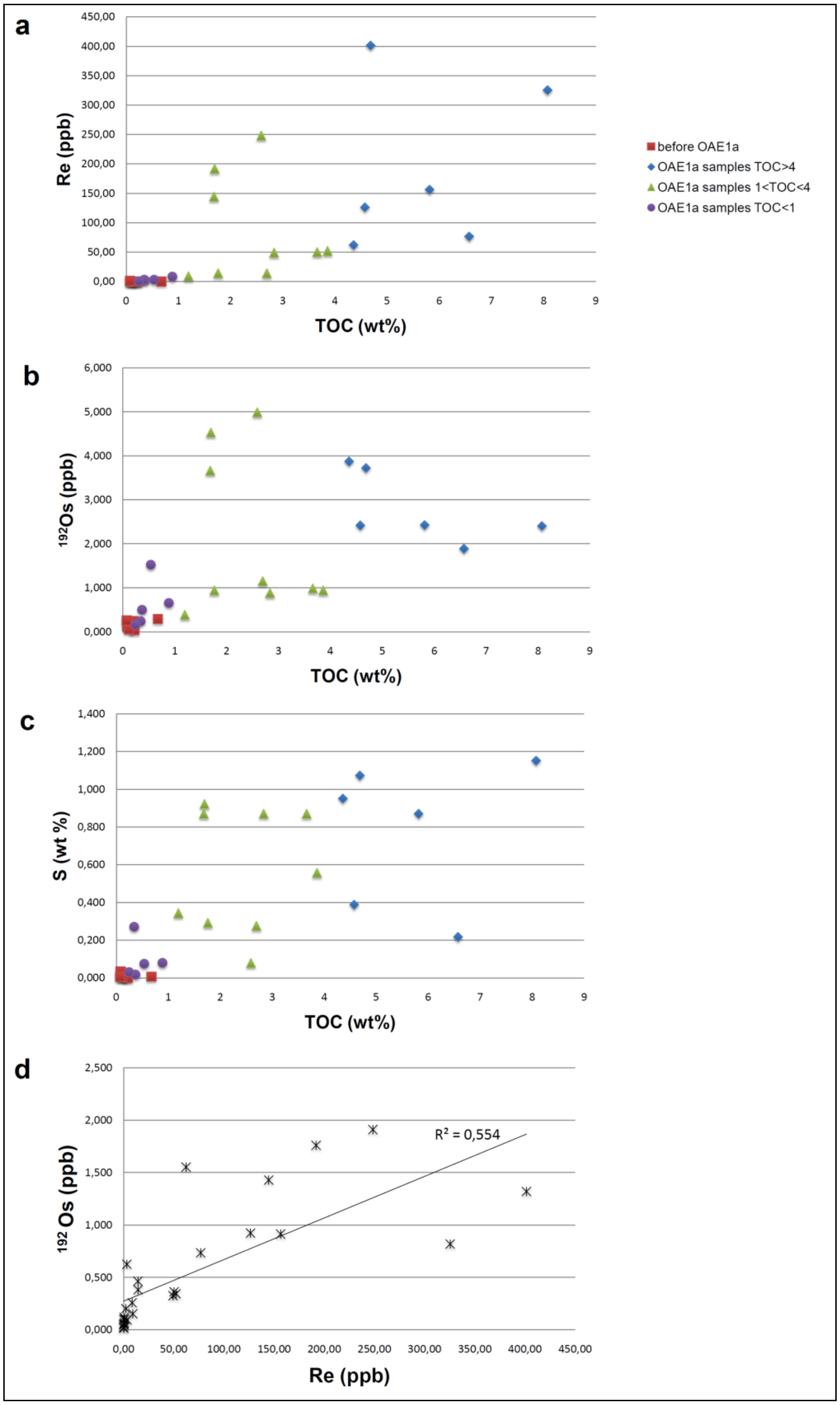

Figure DR2. Variation diagrams showing relationships between (a) TOC and Re concentrations, (b) TOC and ^{192}Os concentrations, (c) S and TOC concentrations and (d) Re and ^{192}Os concentrations, in samples from the Cismon core analysed in this study. In all cases there is a broad but sometimes very poorly defined positive relationship between the parameters displayed.

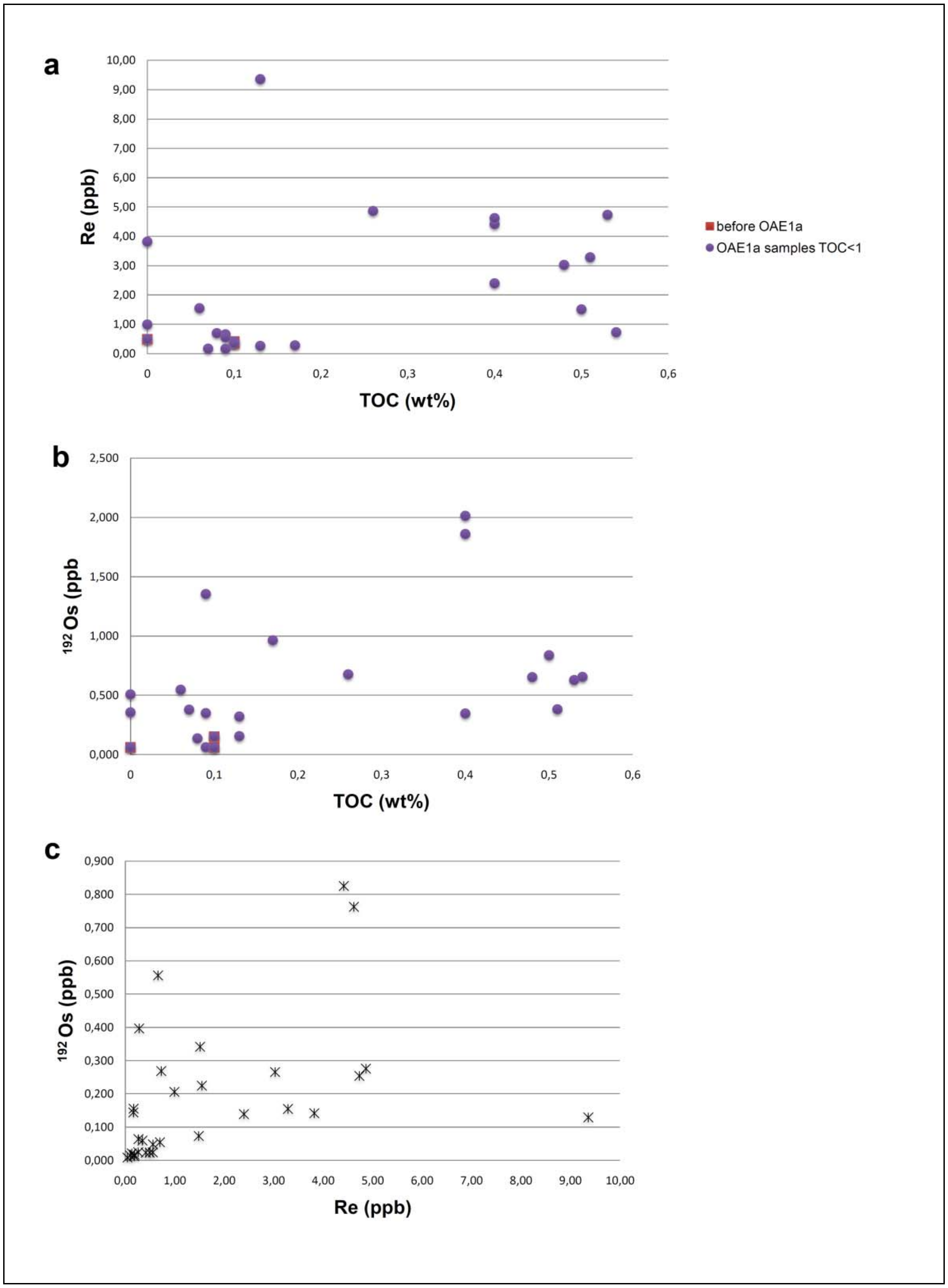

Figure DR3. Variation diagrams showing relationships between (a) TOC and Re concentrations, (b) TOC and ^{192}Os concentrations, and (c) Re and ^{192}Os concentrations, in samples from DSDP Site 463 analysed in this study. There are no clearly defined relationships between these parameters, although the data show broad positive correlations.

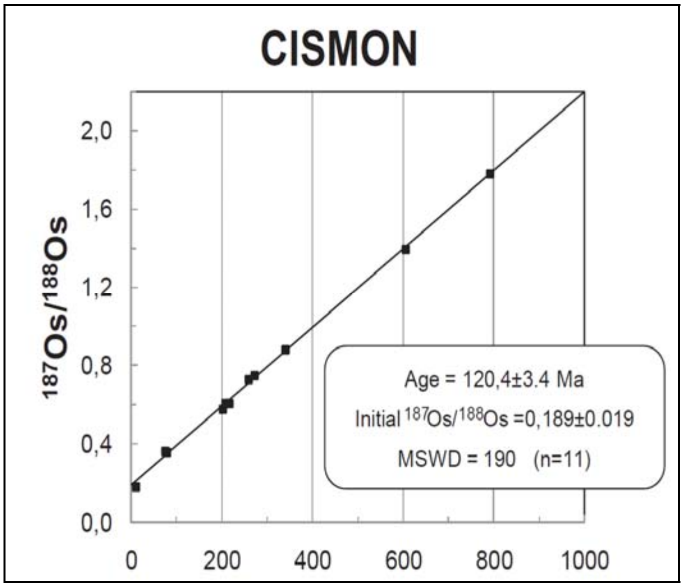

Figure DR4. Re–Os isochron evolution diagram with data from samples from Cismon core.

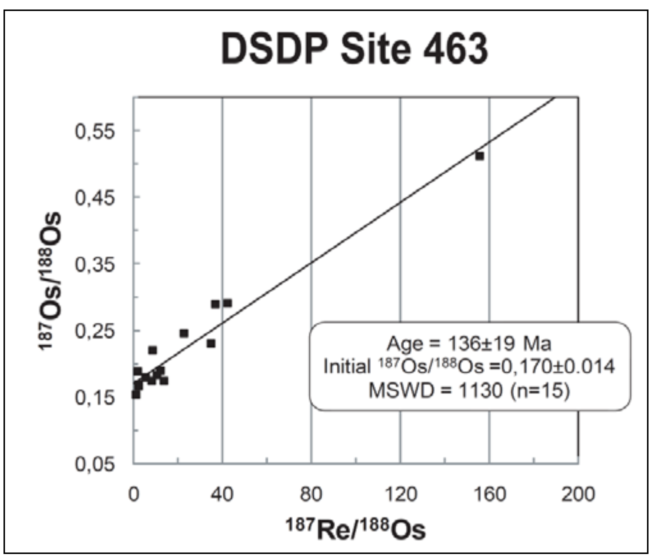

Figure DR5. Re–Os isochron evolution diagram with data from samples from DSDP Site 463.

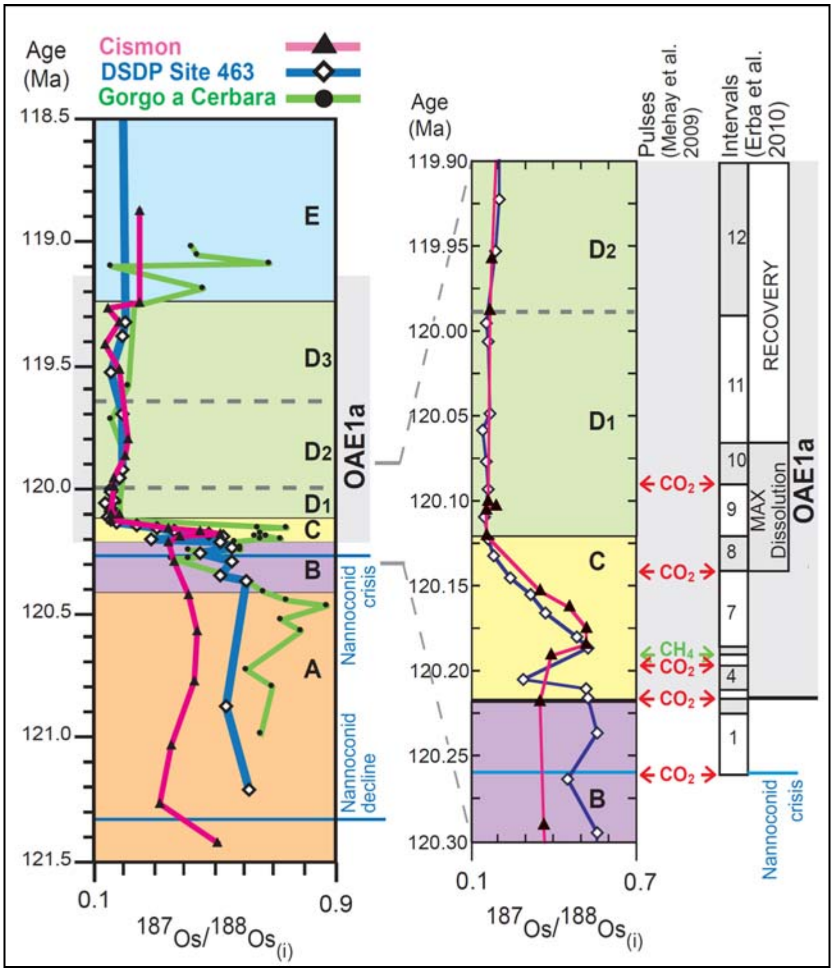

Figure DR6. Correlation between DSDP Site 463, Cismon and Gorgo a Cerbara (Tejada et al., 2009). On the right, close-up of the OAE 1a onset; Os-isotope data are correlated with the CO_2 pulses (Méhay et al., 2009) and intervals of Erba et al. (2010).

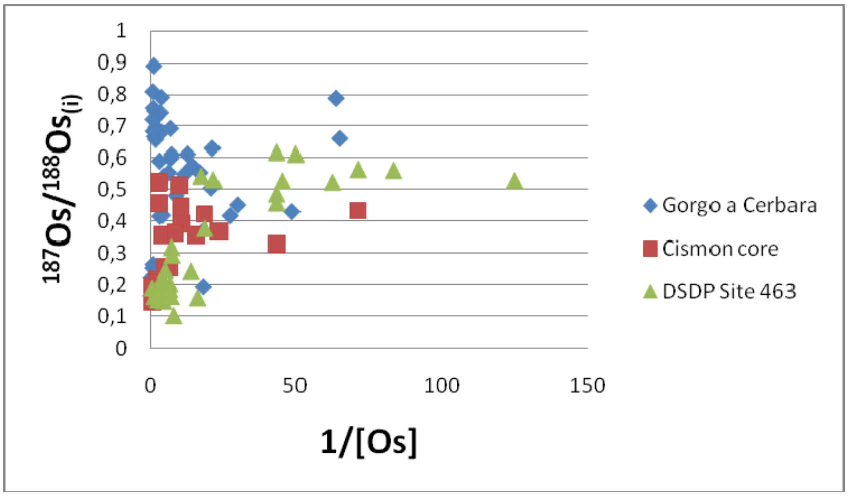

Figure DR7. Isotope mixing diagram showing the initial Os-isotope composition against the reciprocal of the Os abundance for samples from the Cismon core and DSDP Site 463 (this study), and for samples from Gorgo a Cerbara (Tejada et al., 2009).

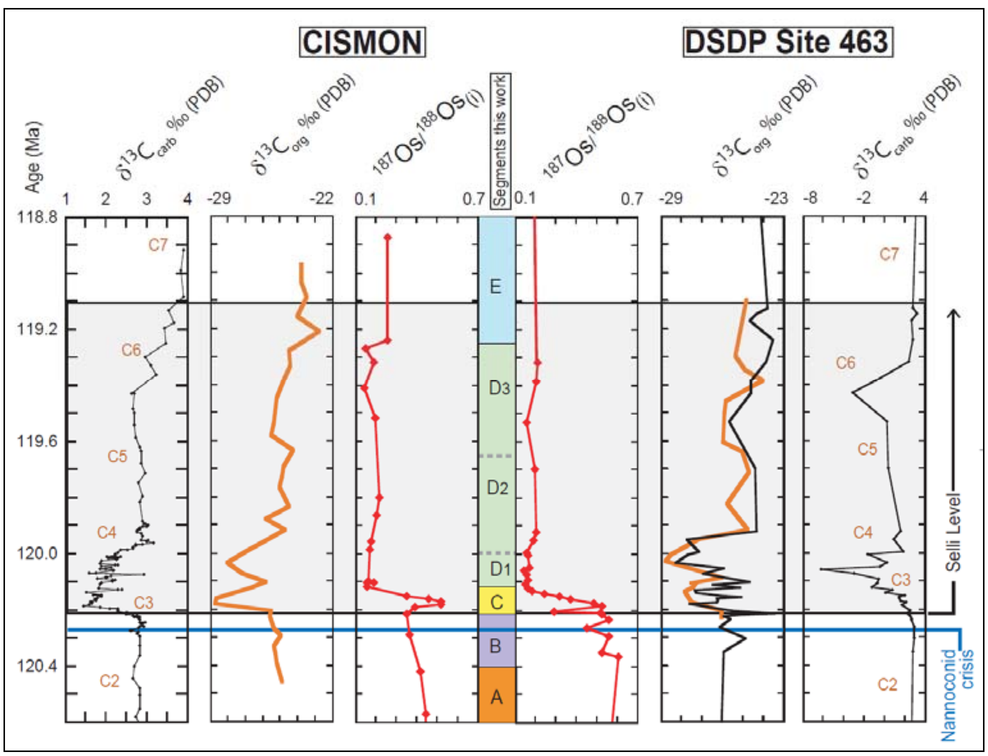

Figure DR8. Stratigraphic correlation between the Cismon core and DSDP Site 463. The correlation is based on $\delta^{13}C_{org}$ values (orange) (Van Breugel et al., 2007) and $\delta^{13}C_{org}$ values (black) from this study. $\delta^{13}C_{carb}$ values for Cismon are from Erba et al. (2010); $\delta^{13}C_{carb}$ values for DSDP Site 463 samples are from this study. The Os-isotope records are shown in red (this study).

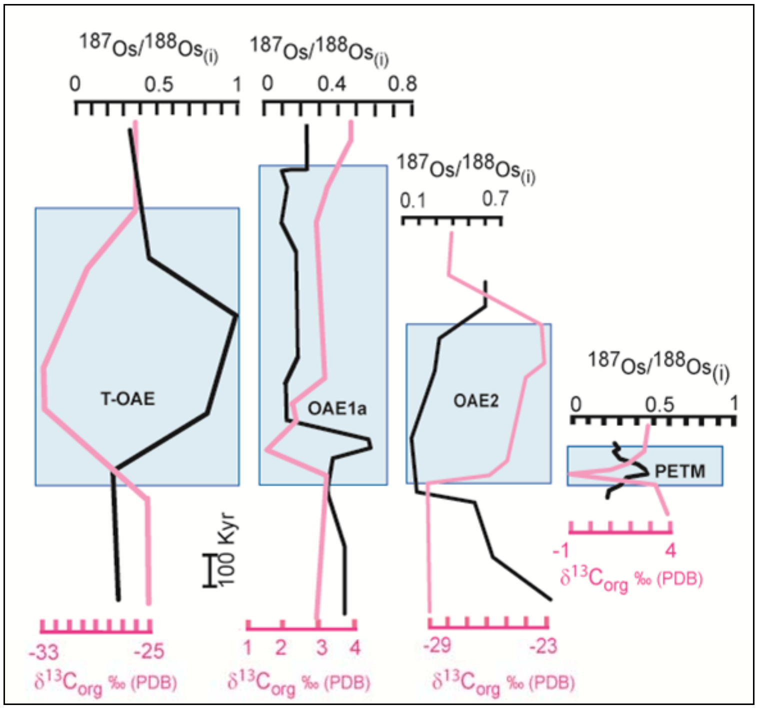

Figure DR9. Os-isotope data against $\delta^{13}C$ for: The Toarcian OAE (T-OAE) (Cohen et al., 2004); OAE 1a (Erba et al., 2010; this study); OAE 2 (Turgeon and Creaser, 2008); and the PETM (Ravizza et al., 2001). Durations are respectively from Suan et al. (2008), Malinverno et al. (2010), Voigt et al. (2008) and Zachos et al. (2005).

Table DR1. Repeat $^{187}Os/^{188}Os$ analyses.

Sample	Age (Ma)	Re (ppb)	Os (ppb)	$^{187}Re/^{188}Os$	$^{187}Os/^{188}Os$	2σ error	$^{187}Os/^{188}Os$ (i)
160_1	119.86	14.180	0.902	78.0	0.36	0.0002	0.207
160_2	119.86	14.640	0.924	78.6	0.36	0.0003	0.207
160_3	119.86	14.450	0.907	79.1	0.37	0.0007	0.209
160_4	119.86	14.314	0.909	78.2	0.36	0.0005	0.208
7a_1	120.09	0.180	0.353	2.5	0.17	0.0011	0.162
7a_2	120.09	0.163	0.337	2.3	0.17	0.0003	0.161
5a_1	120.12	0.350	1.318	1.3	0.17	0.0002	0.167
5a_2	120.12	0.660	1.307	2.4	0.17	0.0001	0.164

Table DR2. Data for Cismon core samples showing their stratigraphic depth (m), calculated age (Ma) (following Malinverno et al., 2010), Re–Os isotope data and elemental abundance data.

Strat. depth (m)	Age (Ma)	$CaCO_3$ (wt%)	TOC (wt%)	S (wt%)	N (wt%)	Re (ppb)	2σ error	Os (ppb)	2σ error	^{192}Os (ppb)	$^{187}Re/^{188}Os$	$^{187}Os/^{188}Os_{(i)}$	$^{187}Os/^{188}Os$	2σ error
17.35	118.876	46.45	0.37	0.02	0.02	2.260	0.0035	0.482	4.18E-07	0.195	23.138	0.258	0.304	0.000418
19.17	119.242	36.83	1.19	0.34	0.03	9.150	0.0171	0.373	6.68E-07	0.147	124.058	0.257	0.504	0.000668
19.29	119.271	34.27	8.08	1.15	0.28	325.500	1.8136	2.323	9.80E-07	0.789	820.278	0.149	1.781	0.000980
19.5	119.321	28.28	4.58	0.39	0.16	126.430	0.1150	2.337	5.81E-07	0.893	281.692	0.189	0.749	0.000581
19.87	119.411	35.55	4.69	1.07	0.17	401.500	0.6674	3.599	8.42E-07	1.276	625.878	0.146	1.392	0.000842
20.32	119.518	7.03	4.36	0.95	0.20	62.260	1.2485	3.739	2.79E-07	1.499	82.598	0.195	0.360	0.000279
21.59	119.800	33.94	2.70	0.28	0.11	14.280	0.0208	1.112	2.31E-07	0.447	63.560	0.216	0.343	0.000231
21.9	119.864	38.48	1.76	0.29	0.06	14.400	0.0178	0.911	4.31E-07	0.366	78.448	0.208	0.364	0.000431
22.36	119.958	44.71	6.57	0.22	0.21	76.820	0.2753	1.827	9.67E-07	0.710	215.176	0.176	0.607	0.000967
22.51	119.988	30.45	5.82	0.87	0.21	156.490	0.5523	2.345	3.83E-07	0.882	352.812	0.172	0.878	0.000383
23.08	120.101	15.06	1.68	0.08	0.06	144.620	1.4109	3.538	4.50E-07	1.381	208.414	0.161	0.579	0.000450
23.09	120.103	14.42	2.59	0.92	0.10	248.440	0.5034	4.821	3.39E-07	1.846	267.570	0.191	0.727	0.000339
23.1	120.105	14.37	1.70	0.87	0.07	191.800	1.6394	4.377	1.47E-06	1.701	224.229	0.158	0.607	0.001473
23.18	120.121	14.04	0.54	0.08	0.02	3.200	0.0078	1.470	1.08E-07	0.603	10.561	0.160	0.182	0.000108
23.34	120.153	20.93	0.89	0.08	0.04	8.480	0.0090	0.631	3.30E-07	0.249	67.764	0.356	0.492	0.000330
23.39	120.163	17.54	2.84	0.56	0.12	49.270	0.0390	0.852	4.61E-07	0.313	313.380	0.457	1.085	0.000461
23.45	120.175	16.59	3.66	0.74	0.17	50.310	0.0260	0.953	7.73E-07	0.350	286.290	0.520	1.094	0.000773
23.5	120.185	24.10	3.86	0.77	0.17	52.250	0.0355	0.911	6.58E-07	0.332	313.243	0.524	1.152	0.000658
23.53	120.191	32.06	0.34	0.27	0.02	3.480	0.0049	0.232	6.25E-07	0.092	75.953	0.392	0.545	0.000625
23.67	120.218	39.81	0.24	0.03	0.01	0.650	0.0018	0.157	4.24E-07	0.063	20.643	0.356	0.397	0.000424
24.18	120.291	65.21	0.12	0.00	0.01	0.120	0.0012	0.104	4.61E-07	0.042	5.608	0.368	0.379	0.000461
25.10	120.422	50.07	0.08	0.03	0.01	0.290	0.0014	0.131	4.02E-07	0.053	11.234	0.423	0.446	0.000402
26.18	120.575	42.16	0.20	0.00	0.04	0.280	0.0589	0.232	6.91E-07	0.093	6.036	0.446	0.458	0.000691
27.59	120.777	87.13	0.22	0.00	0.03	0.290	0.0016	0.035	1.62E-06	0.014	40.839	0.434	0.517	0.001623
29.39	121.029	28.08	0.68	0.01	0.05	0.370	0.0438	0.283	9.91E-07	0.114	6.452	0.364	0.377	0.000991
31.09	121.270	80.87	0.11	0.00	0.03	0.010	0.0021	0.055	2.70E-06	0.023	1.320	0.328	0.330	0.002703
32.43	121.424	25.81	0.07	0.01	0.05	1.120	0.9240	0.251	8.03E-07	0.099	22.705	0.513	0.559	0.000803

Table DR3. Data for DSDP Site 463 samples showing stratigraphic depth (m), calculated age (Ma) (following Malinverno et al., 2010), and Re–Os isotope data.

Core	Section	cm	Strat. depth (m)	N sample	Age (Ma)	Re (ppb)	2σ error	Os (ppb)	2σ error	^{192}Os (ppb)	$^{187}Re/^{188}Os$	$^{187}Os/^{188}Os_{(i)}$	$^{187}Os/^{188}Os$	2σ error
69	CC	7-9	607.57	33	118.05	1.48	0.0022	0.175	3.96E-07	0.071	41.888	0.242	0.324	0.000396
70	1	125-126	614.75	26	119.18	9.36	0.1806	0.309	7.12E-07	0.124	151.002	0.100	0.400	0.000712
70	2	123-125	616.23	18	119.32	4.73	0.0073	0.606	3.30E-07	0.245	38.368	0.213	0.289	0.000330
70	3	39-40	616.89	14	119.39	3.29	0.0549	0.368	1.99E-06	0.149	43.949	0.202	0.290	0.001985
70	3	140-141	617.9	9	119.53	4.86	0.0831	0.653	3.82E-07	0.266	36.362	0.157	0.230	0.000382
70	4	80-82	618.82	4	119.70	3.03	0.0034	0.630	1.48E-07	0.256	23.487	0.199	0.246	0.000148
70	5	60-61	620.1	25a	119.92	1.51	0.0529	0.808	2.48E-07	0.330	9.104	0.202	0.220	0.000248
70	5	123-124	620.73	22a	119.95	142.85	0.1634	4.461	9.16E-07	1.754	161.947	0.188	0.512	0.000916
70	6	59-61	621.59	17a	120.00	4.42	0.0073	1.941	4.50E-07	0.796	11.033	0.160	0.183	0.000450
70	6	81-82	621.81	16a	120.01	4.62	0.0731	1.763	2.21E-07	0.723	12.718	0.163	0.189	0.000221
70	7	7-8	622.57	12a	120.05	0.73	0.0091	0.632	4.47E-07	0.259	5.570	0.168	0.180	0.000447
70	7	19-20	622.69	11a	120.06	1.55	0.0155	0.528	4.69E-07	0.217	14.208	0.146	0.174	0.000469
70	CC	5-6	622.91	10a	120.08	0.27	0.0080	0.149	9.36E-05	0.061	8.622	0.157	0.175	0.093585
71	1	16-18	623.16	7a	120.09	0.16	0.0012	0.337	3.00E-07	0.139	2.338	0.161	0.165	0.000300
71	1	42-43	623.42	6a	120.11	0.28	0.0100	0.950	1.01E-07	0.391	1.419	0.151	0.154	0.000101
71	1	61-62	623.61	5a	120.12	0.66	0.0065	1.307	1.11E-07	0.537	2.444	0.164	0.169	0.000111
71	1	76-78	623.76	4a	120.13	0.17	0.0083	0.364	1.74E-07	0.150	2.235	0.184	0.188	0.000174
71	1	96-97	623.96	3a	120.15	0.99	0.0097	0.481	2.16E-07	0.195	10.122	0.245	0.265	0.000216
71	1	124-125	624.24	2a	120.16	3.82	0.0321	0.344	1.11E-06	0.137	55.515	0.317	0.429	0.001108
71	2	1-3	624.51	78 c	120.17	0.70	0.0023	0.131	4.27E-06	0.053	26.622	0.376	0.429	0.004267
71	2	39-40	624.89	76 c	120.18	0.56	0.0073	0.058	8.89E-07	0.023	48.453	0.485	0.582	0.000889
71	2	58-59	625.08	75 c	120.19	0.56	0.0083	0.118	8.61E-07	0.046	24.068	0.530	0.579	0.000861
71	2	78-80	625.28	74 c	120.21	2.40	0.0035	0.334	3.33E-06	0.134	35.607	0.293	0.365	0.003333
71	2	100-102	625.5	73 c	120.21	0.18	0.0075	0.041	2.19E-06	0.016	22.717	0.522	0.567	0.002185
71	2	120-121	625.7	72 c	120.22	0.04	0.0032	0.019	8.11E-06	0.008	11.035	0.528	0.550	0.008113
71	3	43-46	626.43	68 c	120.24	0.10	0.0050	0.035	2.05E-06	0.014	13.833	0.563	0.591	0.002051
71	3	116-117	627.16	64 c	120.26	0.26	0.0044	0.058	4.67E-06	0.023	22.544	0.457	0.502	0.004667
71	4	7-8	627.57	62 c	120.29	0.18	0.0083	0.030	2.07E-06	0.012	30.484	0.560	0.621	0.002068
71	4	85-87	628.35	58 c	120.35	0.41	0.0117	0.057	6.61E-07	0.022	37.235	0.526	0.601	0.000661
71	CC	7-8	628.56	57 c	120.37	0.13	0.0063	0.051	1.29E-06	0.020	13.111	0.611	0.637	0.001285
72	2	141-142	635.41	40 c	120.88	0.35	0.0035	0.146	1.62E-06	0.057	12.082	0.542	0.567	0.001624
73	2	0-3	643.5	16 c	121.21	0.49	0.0017	0.058	4.39E-06	0.023	43.935	0.617	0.705	0.004390

Table DR4. Carbon stable-isotope data for bulk carbonate and bulk organic-carbon fractions for samples from DSDP Site 463, against stratigraphic depth (m).

CORE	SECTION	cm	m (corrected)	$\delta^{13}C_{carb}$ (‰ PDB)	$\delta^{13}C_{org}$ (‰ PDB)
69	2	105-106	606.55	4.622	
69	2	120-122	606.7	4.527	-24.63
69	3	20-22	607.2	4.546	-24.15
69	3	40-42	607.4	4.388	-24.57
69	CC	7-9	607.57	3.779	-24.84
70	1	77-79	614.27	2.810	-23.76
70	1	96-98	614.46	3.260	-24.29
70	1	125-126	614.75	2.745	-24.65
70	2	40-42	615.4	2.895	-23.51
70	2	123-125	616.23	2.410	-23.83
70	3	39-40	616.89	-0.724	-24.57
70	3	85-87	617.35	-3.067	-24.57
70	3	140-141	617.9	0.322	-25.66
70	4	80-82	618.82	0.373	-24.37
70	5	60-61	620.1	1.674	-24.3
70	5	123-124	620.73	0.915	-27.74
70	6	59-61	621.59	1.900	-27.17
70	6	81-82	621.81	-1.652	-27.69
70	6	141-142	622.41	0.332	-28.29
70	7	7-8	622.57	-0.426	-25.93
70	7	19-20	622.69	-6.149	-26.94
70	CC	5-6	622.91	-2.983	-24.66
71	1	16-18	623.16	-0.478	-26.46
71	1	42-43	623.42	-0.669	-25.15
71	1	61-62	623.61	-1.228	-27.33
71	1	76-78	623.76	0.879	
71	1	96-97	623.96	0.191	-27.3
71	1	124-125	624.24	2.019	-26.04
71	1	138-141	624.38	1.476	-25.04
71	2	1-3	624.51	1.542	-26.29
71	2	19-20	624.69	1.654	-26.2
71	2	39-40	624.89	2.132	-26.3
71	2	58-59	625.08	1.818	-27.64
71	2	78-80	625.28	2.521	-25.55
71	2	120-121	625.7	2.276	-23.43
71	2	140-142	625.9	2.477	-25.29
71	3	0-3	626.0	2.518	-25.95
71	3	43-46	626.43	2.676	-25.59
			626.59	2.708	
71	3	116-117	627.16	3.035	-26.11
71	4	19-20	627.69	2.938	-24.85
71	4	85-87	628.35	2.909	-25.9
72	1	0-3	632.5	2.704	-26.04
72	2	0-6	634.0	3.252	-26.18

Table DR5. Calculated 187Os/188Os(i) for 125 Ma for the first 9 samples from Gorgo a Cerbara (Tejada et al., 2009 original data) compared with the 187Os/188Os(i) calculated for the same samples for 120 Ma.

$^{187}Os/^{188}Os_{(125)}$ (Tejada et al., 2009) AGE 125 Ma	$^{187}Os/^{188}Os_{(120)}$ (Tejada et al., 2009) AGE 120 Ma
0.4289	0.4297
0.4469	0.4500
0.6898	0.6920
0.1595	0.1606
0.4696	0.4797
0.4051	0.4143
0.2515	0.2629
0.2418	0.2519
0.2160	0.2191

Note that the differences in the calculated $^{187}Os/^{188}Os_{(i)}$ are very small, and are insignificant when comparing directly the results of this study with those of Tejada et al. (2009).

References

Bernoulli, D., Jenkyns, H.C., 2009. Ancient oceans and continental margins of the Alpine-Mediterranean Tethys: deciphering clues from Mesozoic pelagic sediments and ophiolites. Sedimentology, v. 56, p. 149–190.

Cohen, A.S., Waters, F.G., 1996. Separation of osmium from geological materials by solvent extraction for analysis by thermal ionisation mass spectrometry. Analytica Chimica Acta v. 332, p. 269-275.

Cohen, A.S., Coe, A.L., Harding, S.M., Schwark, L., 2004, Osmium isotope evidence for the regulation of atmospheric CO_2 by continental weathering: Geology, v. 32, p. 157–160.

Erba, E., 1994, Nannofossils and superplumes: The early Aptian “nannoconid crisis”. Paleoceanography, v. 9, p. 483–501.

Erba, E., Larson, R., 1998. The Cismon Apticore (Southern Alps, Italy): “Reference section” for the Lower Cretaceous at low latitudes. Riv. Ital. Paleontol. Stratigr., v. 104, p. 181-192.

Erba, E., Channell, J.E.T., Claps, M., Jones, C., Larson, R.L., Opdyke, B., Premoli Silva, I., Riva, A., Salvini, G., Torricelli, S., 1999, Integrated stratigraphy of the Cismon APTICORE (Southern Alps, Italy): a reference section for the Barremian-Aptian interval at low latitudes: J. Foraminifer. Res., v. 29, p. 371–391.

Erba, E., Bottini, C., Weissert, J.H., Keller, C.E., 2010, Calcareous Nannoplankton response to surface-water acidification around Oceanic Anoxic Event 1a: Science, v. 329, p. 428–432.

Hay, W.W., 2009, Cretaceous Oceans and Ocean Modeling, In: Cretaceous Oceanic Red Beds: Stratigraphy, Composition, Origins, and Paleoceanographic and Paleoclimatic Significance, SEPM Spec. Pub. v. 91, p. 243–271.

Ludwig, K.R., 1998, ISOPLOT: A Plotting and Regression Program for Radiogenic-Isotope Data, version 2.96.
Malinverno, A., Erba, E., Herbert, T.D., 2010, Orbital tuning as an inverse problem: Chronology of the early Aptian oceanic anoxic event 1a (Selli Level) in the Cismon APTICORE: Paleoceanography, v. 25, PA2203, doi: 10.1029/2009PA001769.
Méhay, S., Keller, C.E., Bernasconi, S.M., Weissert, H., Erba, E., Bottini, C., Hochuli, P.A., 2009, A volcanic CO_2 pulse triggered the Cretaceous Oceanic Anoxic Event 1a and a biocalcification crisis: Geology, v. 37, p. 819–822.
Mélières, F., Deroo, G., Herbin, J.P., 1978. Organic-matter-rich and hypersiliceous Aptian sediments from western Mid-Pacific Mountains. Deep Sea Drilling Project Leg 62, Initial Rep. Deep Sea Drill. Proj., v. 62, p. 903– 915.
Ravizza, G., Norris, R.N., Blusztajn, J., Aubry, M.P., 2001, An osmium isotope excursion associated with the late Paleocene thermal maximum: Evidence of intensified chemical weathering: Paleoceanography, v. 16, p. 155–163.
Roth, P.H., 1981. Mid-Cretaceous calcareous nannoplankton from central Pacific: implications for palaeoceanography. In Initial Reports of the Deep Sea Drilling Project 62 (J. Thiede, T. L. Vallier et al.), p. 471–89. Washington: U.S. Government Printing House.
Roy-Barman, M. and Allegre, C.J., 1995, $^{187}Os/^{186}Os$ in oceanic island basalt: Tracing oceanic crust recycling in the mantle. Earth Planet. Sci. Lett., v. 129, p. 145.
Suan, G., Pittet, B., Bour, I., Mattioli, E., Duarte, L.V., Mailliot, S., 2008, Duration of the Early Toarcian carbon isotope excursion deduced from spectral analyses: Consequence for its possible causes: Earth and Planetary Science Letters, v. 267, p. 666–679.
Tejada, M.L.G., Katsuhiko S., Kuroda, J., Coccioni, R., Mahoney, J.J., Ohkouchi, N., Sakamoto, T., Tatsumi, Y., 2009, Ontong Java Plateau eruption as a trigger for the early Aptian oceanic anoxic event: Geology, v. 37, p. 855–858.
Thiede, J., Dean, W.E., Rea, D.K., Vallier, T.L., Adelseck C.G., 1981. The geologic history of the Mid-Pacific Mountains in the central North Pacific Ocean: A synthesis of deep-sea drilling studies. Iniz. Rep. Deep Sea Drill. Proj. v. 62, p. 1073-1120.
Turgeon, S.C. and Creaser, R.A., 2008, Cretaceous oceanic anoxic event 2 triggered by a massive magmatic episode: Nature, v. 454, p. 323–326.
Voigt, S., Erbacher, J., Mutterlose, J., Weiss, W., Westerhold, T., Wiese, F., Wilmsen, M., Wonik, T., 2008, The Cenomanian–Turonian of the Wunstorf section–(north Germany): Global stratigraphic reference section and new orbital time scale for oceanic anoxic event 2: Newsl. Stratigr., v. 43, p. 65–89, doi: 10.1127/0078-0421/2008/0043-0065.
Weissert, H., Lini, A., 1991. Ice Age interludes during the time of Cretaceous greenhouse climate? In Controversies in Modern Geology. Edited by D.W. Muller, J.A. McKenzie and H. Weissert, Academic, San Diego, Calif., p. 173-191.
Zachos, J.C. et al., 2005, Rapid acidification of the Ocean during the Paleocene-Eocene Thermal Maximum: Science, v. 308, p. 1611.